Journal of Orthopaedic Translation (2019) 19, 81—93

Available online at www.sciencedirect.com

ScienceDirect

journal homepage: http://ees.elsevier.com/jot

ORIGINAL ARTICLE

Effect of porous tantalum on promoting the osteogenic differentiation of bone marrow mesenchymal stem cells *in vitro* through the MAPK/ERK signal pathway

Xiaojie Dou [a,☆], Xiaowei Wei [b,☆], Ge Liu [b], Shuai Wang [c], Yongxiang Lv [a], Junlei Li [b], Zhijie Ma [a], Guoshuang Zheng [b], Yikai Wang [a], Minghui Hu [a], Weiting Yu [b], Dewei Zhao [a,*]

[a] *Department of Orthopedics, Affiliated Zhongshan Hospital of Dalian University, Dalian, Liaoning, China*
[b] *Laboratory of Orthopedics, Affiliated Zhongshan Hospital of Dalian University, Dalian, Liaoning, China*
[c] *Department of Orthopedics, Binzhou People's Hospital, Binzhou, Shandong, China*

Received 24 October 2018; received in revised form 2 March 2019; accepted 18 March 2019
Available online 15 April 2019

KEYWORDS
Bone marrow mesenchymal stem cells;
Cytocompatibility;
MAPK/ERK signaling pathway;
Osteogenic differentiation;
Porous tantalum

Abstract *Background:* As an ideal new graft material, porous tantalum (pTa) has excellent mechanical properties and corrosion resistance and has received increased attention in the biomedical field because of its excellent cytocompatibility and ability to induce bone formation. However, the molecular mechanism of its potential to promote osteogenesis remains unclear, and very few reports have been published on this topic.
Methods: In this study, we first produced porous Ti6Al4V (pTi6Al4V) and pTa with the same pore size by three-dimensional printing combined with chemical vapour deposition. The number of adhesions between pTa and pTi6Al4V and bone marrow mesenchymal stem cells (BMSCs) after 1 day of culture was detected by the live/dead cell staining method. The proliferation activity of the two groups was determined after culture for 1, 3, 5 and 7 days by the cell counting kit-8 method. In addition, the osteogenic activity, mRNA expression levels of osteogenic genes alkaline phosphatase (ALP), osterix (OSX), collagen-I (Col-I), osteonectin (OSN) and osteocalcin (OCN) and protein expression levels of the mitogen-activated protein kinase/extracellular signal-regulated kinase (MAPK/ERK) signalling pathway marker p-ERK of the two groups cultured for 7, 14 and 21 days were determined by the ALP activity assay, real-time quantitative polymerase chain reaction (Q-PCR) and Western blotting, respectively. Subsequently, the

* Corresponding author. Affiliated Zhongshan Hospital of Dalian University, NO. 6 Jiefang Street Zhongshan, District, Dalian, 116001, China.
E-mail address: zhaodewei2016@163.com (D. Zhao).
☆ The first two authors contributed equally to this work

https://doi.org/10.1016/j.jot.2019.03.006

two groups were treated with the MAPK/ERK—specific inhibitor U0126, and then, the mRNA expression levels of osteogenic genes and protein expression levels of p-ERK in the cultures were determined by Q-PCR and Western blotting, respectively.
Results: The live/dead cell staining and cell counting kit-8 assays showed that the adhesion and proliferation activities of BMSCs on pTa were significantly better than those on pTi6Al4V. In addition, the ALP activity assay and Q-PCR showed that pTa harboured osteogenic activity and that the osteogenic genes ALP, OSX, Col-I, OSN and OCN were highly expressed, and by Western blotting, the expression of p-ERK protein in the pTa group was also significantly higher than that in the pTi6Al4V group. Subsequently, using the MAPK/ERK—specific inhibitor U0126, Western blotting showed that the expression of p-ERK protein was significantly inhibited and that there was no difference between the two groups. Furthermore, Q-PCR showed that osteogenic gene expression and ALP expression levels were significantly increased in the pTa group, and there were no differences in the OSX, Col-I, OSN and OCN mRNA expression levels between the two groups.
Conclusion: Overall, our research found that compared with the widely used titanium alloy materials, our pTa can promote the adhesion and proliferation of BMSCs, and the molecular mechanism of pTa may occur via activation of the MAPK/ERK signalling pathway to regulate the high expression of OSX, Col I, OSN and OCN osteogenic genes and promote the osteogenic differentiation of BMSCs *in vitro*.
The translational potential of this article: Our self-developed pTa material produced by three-dimensional printing combined with the chemical vapour deposition method not only retains excellent biological activity and osteoinductive ability of the original tantalum metal but also saves considerably on material costs to achieve mass production of personalised orthopaedic implants with pTa as a stent and to accelerate the wide application of pTa implants in clinical practice, which have certain profound significance.

Introduction

Osteonecrosis is a common disease in orthopaedics, and the most common site of necrosis is the femoral head. If treatment of osteonecrosis of the femoral head (ONFH) is not timely, it will lead to structural changes of the femoral head, collapse of the femoral head, deformation and finally the formation of inflammation of the joints, resulting in walking dysfunction and seriously affecting the quality of life of patients. Presently, ONFH treatment is mainly divided into nonsurgical treatment and surgical treatment. Surgical treatment is divided into hip-preserving surgery and artificial total hip arthroplasty. Although artificial total hip arthroplasty can restore the patient's function in a short time, problems such as secondary revision are also encountered. Particularly for young and middle-aged patients, the number of premature joint replacement surgeries is much higher than expected. To avoid or delay the replacement of artificial joints as much as possible, head-fixing surgery for avascular necrosis of the femoral head in young adults is increasingly used in clinical practice. Preserved femoral head surgery includes core decompression, bone grafting, osteotomy and bone grafting with or without blood transport [1]. However, these treatment methods are associated with their respective limitations. Therefore, in the treatment of osteonecrosis, we are still exploring new methods that can block the process of pathological necrosis and prevent the collapse of osteonecrosis. With a many clinical and scientific research advances, bone tissue engineering has developed rapidly, and the application of tissue engineering methods to repair osteonecrosis has become a hot spot [2,3]. Biomaterials are one of the main components in tissue engineering. Ideal orthopaedic biomaterials need to provide not only sufficient mechanical support but also good biocompatibility and osteoinductive capacity [4]. In bone tissue engineering, decalcified bone matrix, poly(-lactic acid) (PLA), polyethanolide and its copolymers, bioceramics, etc. The decalcified bone matrix materials have almost been eliminated because of their relatively complicated preparation process and insufficient mechanical strength. When PLA, poly (ethanolic acid) and its copolymers were used, the rate of self-absorption of the material matched with the rate of new bone formation, which could provide scaffold for bone growth and hardly interfere with the shaping of new bone at the same time. However, with the increasing use of polymer materials, their hydrophilicity is poor, immune reaction occurs easily around the implants, there is lack of sufficient mechanical stiffness and the degradation rate is difficult to control. This series of problems also greatly reduced the scope of application of this material. In addition, researchers have also developed a variety of bioceramic materials, which have clear advantages and good biocompatibility with human tissues. In many experiments, it has been proved that this material can easily form a good bony bond with the broken end of the implanted bone, but the defects of the material are obvious: its brittleness is large, its shape is difficult and it is difficult to be sintered; so, its application has been greatly restricted. These materials limit

their application in the treatment of osteonecrosis because of their respective shortcomings [5,6].

With the continuous improvement of industrial technology, the development of metal-based artificial biomaterials has developed rapidly. Four major materials, stainless steel, cobalt—chromium alloy, titanium alloy and tantalum (Ta), have emerged. Although stainless steel is low in manufacturing cost, it lacks coordination with the host bone compared with the other metal materials, and its surface does not provide bone tissue attachment or osseointegration [7]. In addition, cobalt—chromium alloy has a modulus of elasticity of 220 GPa, greatly limiting its use. Presently, the most commonly used Ti6Al4V alloy material is widely used in clinical practice because of its low density, high strength, excellent corrosion resistance and low cost. However, in the elastic modulus test, although the elastic modulus of titanium alloy (110 GPa) has been reduced by much more than that of the cobalt—chromium alloy [8], it is still much higher than the elastic modulus of human bone (cortical bone 2—30 GPa and cancellous bone 0.01—3 GPa). In addition, because its tensile strength, compressive strength and flexural strength are much higher than those of human bone, when the titanium alloy is implanted into the body subjected to mechanical action, the force will be blocked by the material to produce a stress-shielding effect and cause looseness or even breakage. To this end, clinicians and materials science experts have begun to use porous structures to replace dense materials and have achieved preliminary results [9]. However, titanium alloy is not biologically active; the combination of the material and bone is dependent on mechanical fitting; the bonding strength after implantation is insufficient and it is still prone to loosening and operation failure. Subsequently, when metal materials were sought with an elastic modulus similar to that of human bone and with osseointegration ability, Ta and porous tantalum (pTa) were identified. Scholars have carried out many animal experiments and clinical applications, and the results have shown that the elastic modulus of pTa (0.1—30 GPa) lies between that of cortical bone and cancellous bone, indicating that it can reduce the stress shielding of bone and shows superior biocompatibility, osteoinductive ability and good biomechanical properties; it has become a hot topic at home and abroad [10—12]. However, pTa induces stem cell osteogenesis and molecular mechanisms, especially compared with the nonbiologically active, traditional porous Ti6Al4V (pTi6Al4V); current research reports on this issue are rare.

Another important aspect of tissue engineering is the selection of seed cells [4]. Presently, various cell types can be selected as seed cells. When selecting seed cells, the number of cells and difficulty of extraction need to be prioritised, and the biological activity, differentiation potential and immune response of the cells need to be strictly controlled. Bone marrow mesenchymal stem cells (BMSCs) are ideal candidates for bone tissue engineering seed cells. In recent years, studies have shown that BMSCs have broad plasticity, are exposed to different microenvironments and can recombine and differentiate into cells of all three germ layers, osteoblasts, endothelial cells, chondrocytes and fibroblasts [13,14], making it a popular tissue engineering seed cell type. In addition, because of its convenient access, wide source, easy separation and culture, retention of stem cell characteristics after multiple passages, lack of immunological rejection, multidirectional differentiation potential and strong proliferative capacity, it has received the most extensive attention of researchers [15—17]. Our previous study also found that the use of autologous BMSCs combined with pTa rod implantation and vascularised iliac grafting for the treatment of end-stage ONFH can effectively delay or avoid total hip arthroplasty [18]. Thus, after autologous stem cells are combined with pTa, does osteogenic induction of pTa or the response of stem cells to other inducing factors occur in the body? Therefore, we used BMSCs to attempt to explain the potential molecular mechanisms of the biocompatibility and osteoinductive properties of pTa by adhesion, proliferation and differentiation of stem cells.

Mitogen-activated protein kinases (MAPKs) are a family of intracellular serine/threonine protein kinases that transmit signals from the cell surface to the nucleus in response to various stimuli, including surface structures, hormones, chemicals and stress, and they play a vital role in the process of causing cellular biological responses such as cell proliferation, differentiation, transformation and apoptosis [19]. Previous studies have shown that the MAPK signalling pathway uses three major pathways—MAPK/ERK, MAPK/Jun N-terminal kinase (JNK) and MAPK/P38—in which the MAPK/ERK signalling cascade regulates gene expression to regulate proliferation, differentiation and apoptosis, among which the regulation of osteogenic differentiation of mesenchymal stem cells is closely related [20]. Zhang et al [21] found that strain-induced osteogenic differentiation of OVX BMSCs may occur via the ERK1/2-MAPK signalling pathway but not the p38 or JNK-MAPK signalling pathway. Cao et al [22] considered that titanium-supported silver nanoparticles promote BMSC osteogenesis by activating the MAPK/ERK signal cascade. In this study, we primarily investigated whether MAPK/ERK is involved in the regulation of the osteogenic differentiation of BMSCs.

Therefore, using the biological characteristics of BMSCs, the clinically widely used Ti6Al4V was selected as the control material, and the same pores and shapes of pTi6Al4V and pTa were prepared by three-dimensional (3D) printing combined with chemical vapour deposition (CVD). Subsequently, we observed the differentiation of the pTa composite BMSCs *in vitro* and explored their mechanism of action to provide a theoretical basis for the clinical application of pTa combined with autologous BMSCs in the treatment of osteonecrosis, bone defects and other clinical applications [23,24].

Materials and methods

Preparation of materials

Both pTi6Al4V and pTa were prepared autonomously by the Laboratory of Orthopedics of the Affiliated Zhongshan Hospital of Dalian University [25]. The dimensions were designed as follows: the solid column beam size was 600 μm, and the aperture was 500 μm. The sample was always printed on a titanium alloy substrate under argon filling protection throughout the preparation of the porous

scaffold, and then the sample was separated from the substrate by a wire electrodischarge machining (EDM) technique. A cylindrical body with a diameter of 20 mm and a height of 30 mm was prepared, and it was cut into a cylindrical sheet with a diameter of 20 mm and a thickness of 1 mm. After the preparation was completed, all the samples were sequentially subjected to sand blasting and ultrasonic cleaning to remove the residual metal powder in the porous structure and oxide layer of the surface layer of the material to obtain a porous titanium alloy. Subsequently, for the pTa group, the surface coating was applied by the CVD method on the pTi6Al4V sheet, a titanium alloy was used as a support and the surface was covered with a 20-μm-thick Ta-coated metal sheet. The composition of the samples was examined by scanning electron microscopy (JSM-6360LV, JEOL, Tokyo, Japan) to observe the pore size of the two materials and size of the beam.

Isolation and culture of BMSCs

All the procedures on animals were approved by the Animal Ethics Committee of Dalian University. The use of animals was approved by the Institution's Animal Care and Use Committee. BMSCs were obtained from 6 healthy 3-week-old Sprague—Dawley (SD) rats, male or female, provided by the Animal Center of Dalian Medical University. Through the whole bone marrow culture, BMSCs were obtained by periodically changing fluids to remove nonadherent cells according to the characteristics of growth of haematopoietic cells by adherent growth of BMSCs. Whole bone marrow was pooled and resuspended in culture medium (DME/F12, HyClone; Thermo Fisher Scientific, Waltham, MA, USA), containing 10% fetal bovine serum (FBS) (HyClone; Thermo Fisher Scientific, Waltham, MA, USA), 100 UI/mL of penicillin (Invitrogen; Life Technologies, Carlsbad, CA, USA) and 100 mg/mL of streptomycin (Invitrogen; Life Technologies, Carlsbad, CA, USA), and then was seeded on cell culture plastic dishes. The cells were maintained at 37°C under 5% CO_2 in humidified air. After 48 h, the cultures were rinsed carefully with phosphate-buffered saline (PBS, HyClone; Thermo Fisher Scientific, Waltham, MA, USA) to remove nonadhered cells and were cultured in fresh culture medium. After 10—12 days, the cells reached approximately 90% confluence, which were used for subsequent experimental studies.

Flow cytometry

The third-generation well-grown cells were collected, washed 2 times with PBS, harvested and counted. Then, 5×10^5 cells in 100 μL of PBS were incubated with 5 μL of P-phycoerythrin (PE)-conjugated mouse anti-rat CD44 (0.2 mg/mL), 5 μL of fluorescein isothiocyanate (FITC)-conjugated mouse anti-rat CD90 (0.2 mg/mL) and 5 μL of FITC-conjugated rabbit anti-rat CD45 (0.2 mg/mL) for 15 min. The negative control was generated by replacing the antibody with isotype IgG. After washing with PBS containing 1% BSA (Sigma-Aldrich; St. Louis, MO, USA), the fluorescence of cells was analysed using a Coulter EPICS XL flow cytometer (Beckman Coulter; Fullerton, CA, USA).

Scaffold cell loading and fluorescence labelling

The two sets of materials were transferred to a new 12-well plate and gently washed 2—3 times with 1 mL of PBS. Then, 5 μL of calcein AM (component A) and 20 μL of EthD-1 (component B) from the live/dead reagent kit (Sigma-Aldrich; St. Louis, MO, USA), at room temperature, were prepared in 10 mL of PBS to produce a staining solution (2 μM calcein AM and 4 μM EthD-1), and 1 mL of this diluted staining solution was added to the two groups of materials. In the medium, the cells were incubated for 10 min at room temperature, and the cell state and adhesion amount of the two groups of materials were observed under a fluorescence microscope.

Cell counting kit-8 proliferation assay

The stent was placed in a 12-well plate, rat BMSCs were inoculated on the stent at a seeding density of 5×10^4/well and the medium was replaced with fresh medium every 2 days. Three parallel groups of pTa and pTi6Al4V and four time points, 1, 3, 5 and 7 days, were used. Each group had 3 pieces of material at each time point, and the cells were placed in an incubator at 37°C and 5% CO_2. After 1, 3, 5 and 7 days of culture, the medium was aspirated at each time point, washed twice with 1 mL of PBS and replaced with fresh medium containing 10% cell counting kit-8 (CCK-8; Dojindo, Kumamoto, Kyushu, Japan) reagent. The cells were allowed to react in a 5% CO_2, 37°C incubator for 2 h, and then 100 μL of the medium containing 10% CCK-8 reagent was removed from each sample and transferred to a 96-well plate to measure the absorbance at 450 nm.

Alkaline phosphatase activity assay and osteogenic mineralised nodule staining

Alkaline phosphatase (ALP) activity was tested using p-nitrophenyl phosphate (pNPP; Biyuntian, Nanjing, Jiangsu, China) to test the osteogenic differentiation ability of BMSCs on material scaffolds. The scaffolds were placed in a 12-well plate, SD rats' BMSCs were inoculated on the material and the seeding density was 1.5×10^5/well. On the second day, the material was turned over and reinoculated with the same amount of BMSCs as that on the first day. On the third day, the materials of the BMSCs inoculated on the front and back were carefully transferred to a new 12-well plate, and the medium was replaced with fresh medium every 2 days. Starting with the second inoculation of BMSCs, after the cells were cultured with materials for 7, 14 and 21 days, the culture solution was discarded and the cells and materials were gently washed 3 times with PBS and digested with 0.5 mL/well of 0.25% trypsin for 2—3 min to neutralise the medium. Then, the cells were transferred to a 15-mL tube and were centrifuged at 1800 r/min for 8 min, followed by discarding the supernatant and mixing the cell pellet with 1 mL of PBS by pipetting. The cell suspension was transferred to a 1.5-mL eppendorf (EP) tube and was centrifuged again at 1800 r/min for 8 min. The supernatant was carefully discarded and the pellet was placed on crushed ice, lysed with 50 μL of cell lysate buffer (Biyuntian, Nanjing; Jiangsu, China) and centrifuged at 12000 r/

min for 5 min at 4°C. Thereafter, the supernatant was transferred to a new tube, and 35 μL of the supernatant was mixed with 100 μL of the ALP substrate reaction solution and was placed at 37°C in the dark. After 30 min of reaction, 100 μL of the stop solution was added to terminate the reaction. The ALP activity was determined by measuring the absorbance at a wavelength of 405 nm using a microplate reader, the total protein content was measured using a bicinchoninic acid (BCA) protein concentration assay kit (Nanjing Keygen Biotech Co., Ltd., Jiangsu, China) and the measured optical density (OD) value was converted to the corresponding total protein content ratio according to the conversion formula provided in the kit.

Alizarin red staining—light microscope observation of mineralised nodules

pTa and pTi6Al4V scaffolds were placed in a 12-well plate, and the third-generation SD rat BMSCs were inoculated on the scaffolds with a density of 5×10^4/well. The cells were observed every day and cultured continuously for 21 days. The culture medium was absorbed carefully, fixed with 4% paraformaldehyde (Cyagen Biosciences Inc, Guangzhou, China) for 60 min and washed twice with PBS; 0.1% alizarin red dye solution was added and stained for 30 min, followed by washing twice with PBS, which was observed and photographed under a light microscope.

Tetracycline staining—laser confocal microscope observation of mineralised nodules

pTa and pTi6Al4V scaffolds were placed in 12-well plates, and the third-generation SD rat BMSCs were inoculated on the scaffolds with a density of 5×10^4/well. One percent tetracycline fluorescence solution (Leagene, Beijing, China) was added to the culture medium. The cells were observed, and the medium exchanged every day. After continuous culture for 21 days, the culture medium was carefully sucked out and washed by PBS. After fixing with 4% paraformaldehyde for 15 min, it was washed twice with PBS, and 4′,6-diamidino-2-phenylindole (DAPI) was added to the nuclear lining for 8 min, washed twice with PBS, observed under a fluorescence microscope and photographed.

Real-time quantitative polymerase chain reaction analysis

Real-time quantitative polymerase chain reaction (Q-PCR) was used to detect the osteogenic differentiation of SD rat BMSCs. The scaffolds were placed in a 12-well plate, SD rat BMSCs were inoculated on the material and the seeding density was 1.5×10^5/well. On the second day, the material was turned over and reinoculated with the same amount of BMSCs as the first day. On the third day, the materials of the BMSCs inoculated on the front and back were carefully transferred to a new 12-well plate, and the medium was replaced with fresh medium every 2 days. After 7, 14 and 21 days, Q-PCR detected the expression levels of ALP, osterix (OSX), collagen-I (Col-I), osteonectin (OSN) and osteocalcin (OCN). Total RNA was extracted from the cells on the scaffold at each time point using RNAiso Plus (TaKaRa; Dalian, Liaoning, China) and then was converted to cDNA using the PrimeScriptTM RT Master Mix (TaKaRa, Dalian, Liaoning, China). The expression level of the relevant osteogenic gene markers was determined by Sybr Green using a Q-PCR instrument (Applied Biosystems, Carlsbad, CA, USA). The reaction parameters were set to 95°C for 30 s, 95°C for 5 s for 40 cycles and 60°C for 34 s. Glyceraldehyde-3-phosphate dehydrogenase (GAPDH) served as a housekeeping gene. The expression levels of the aforementioned osteogenesis-related genes were calculated by normalising the value to that of the housekeeping gene based on the $2^{-\Delta\Delta CT}$ method. Primer sequences are shown in Table 1.

To measure the expression of the MAPK/ERK pathway protein, cells were harvested for 7, 14 and 21 days after culture of BMSCs with pTa and pTi6Al4V. The samples collected by trypsinization were lysed in radio immunoprecipitation assay (RIPA) lysis buffer (Biyuntian; Nanjing, Jiangsu, China) containing 1 mM phenylmethylsulfonyl fluoride (PMSF; Biyuntian; Nanjing, Jiangsu, China) and 1 mM phosphatase inhibitor according to the manufacturer's instructions. The protein concentration was measured using the BCA protein assay. Each 20 μg of the protein was loaded onto a 12% sodium dodecyl sulfate-polyacrylamide gel electrophoresis (SDS-PAGE) gel for electrophoresis and then was transferred to a 0.45-μm polyvinylidene fluoride (PVDF) membrane (Millipore; Boston, MA, USA) at 200 mA in a blotting apparatus (Bio-Rad, Hercules, CA, USA) for 1.5 h. The membrane was allowed to react with blocking solution (Nanjing Keygen Biotech Co., Ltd., Jiangsu, China) for 2 h at room temperature and with the primary antibodies ERK (CST; Boston, MA, USA), P-ERK (CST; Boston, MA, USA) and GAPDH (CST; Boston, MA, USA). Then, the membrane was washed in tris buffered saline and Tween (TBST) for 10 min, 3 times, and then was incubated for 1 h at 37°C with the secondary antibody (CST; Boston, MA, USA). Finally, the membrane was again washed in TBST for 10 min, 3 times, followed by development using an automatic fluorescent

Table 1 The primer sequence of Q-PCR.

Genes	Primers	Sequences (5′—3′)
ALP	Forward	CGAGCAGGAACAGAAGTTTGC
	Reward	GAATCCGACCCACGGAGG
OSX	Forward	GCCTACTTACCGTGACTTT
	Reward	GCCCACTATTGCCAACTGC
Collagen I	Forward	GACATGTTCAGCTTTGTGGACCTC
	Reward	GGGACCCTTAGGCCATTGTGTA
OSN	Forward	GCCCGAGACTTTGAGAAGAACTAC
	Reward	GATGTCCTGCTCCTTGATGC
OCN	Forward	GGTGGTGAATAGACTCCGGC
	Reward	AGCTCGTCACAATTGGGGTT
GAPDH	Forward	GAAGGCAGCCCTGGTAACC
	Reward	ATGGTGGTGAAGACGCCAGTAA

ALP = alkaline phosphatase; OSX = osterix; OSN = osteonectin; OCN = osteocalcin; Q-PCR = real-time quantitative polymerase chain reaction.

chemiluminescence instrument (Tanon; Shanghai, China) and the electrochemiluminescence (ECL) chemiluminescence kit (Abbkine; Redlands, CA, USA). GAPDH was evaluated three times in this experiment as an internal control. Image-Proplus 6.0 software (Media Cybernetics, MD, USA) was used for grayscale analysis.

EKR1/2 inhibition study

To further identify whether the MAPK/ERK signalling pathway was involved in the osteogenic differentiation of BMSCs, the effect of EKR1/2 inhibition on BMSC osteogenesis-specific gene expression was evaluated, and BMSCs were cultured with pTa and porous titanium. Of the four groups, two groups with pTa and pTi6Al4V were cultured for 7 days, serving as the control groups, and the other two groups were treated with 10 μM U0126 (CST; Boston, MA, USA), followed by culture for 7 days. The proteins were collected after lysing the cells on day 7, and the protein expression levels of p-ERK1/2, ERK1/2 and GAPDH of each group of materials were determined. As described previously, the protein expression of p-ERK, ERK, and GAPDH\ was measured on the 7th day, followed by total RNA extraction in the inhibition group, and then the ALP, OSN, Col-I and OSX expression was assessed after treatment with the inhibitor by Q-PCR. The relative mRNA expression level of OCN was also determined.

Statistics

Statistical processing was performed using SPSS 20.0 software (IBM, NY, USA). All experiments were repeated at least 3 times. The data were presented as means ± standard deviation, and independent sample *t* test or one-way analysis of variance was used to compare between groups. A p value < 0.05 was considered statistically significant.

Results

Scanning electron microscopy observation of material appearance and composition

Scanning electron microscopy showed that the surface morphology of pTa and pTi6Al4V and the surface element analysis results energy dispersive spectrometer (EDS) of the two sets of materials were cylindrical pieces with a diameter of 20 mm and a thickness of 1 mm. Figure 1A shows pTa, and Figure 1D shows pTi6Al4V. Figure 1B and E and Figure 1C and F show the surface composition of pTa and pTi6Al4V, respectively, analysed by energy spectrum analysis.

Identification of BMSCs by flow cytometry

The isolated cells expressed the BMSC marker CD44 (Figure 2B) and CD90 (Figure 2D) but scarcely expressed the haematopoietic stem cell marker CD45 (Figure 2E). In addition, Figure 2A shows the PE negative control, and Figure 2C shows the FITC negative control. These BMSC expression patterns in the rat are similar to those in humans.

Adhesion of BMSCs on pTa or -pTi6Al4V

After 48 h, the adherent cells from the primary culture system exhibited a round, elliptical or polygonal shape, some of which began to stretch. After 10 days, BMSCs reached approximately 90% confluence (Figure 3A). After the third passage, the cells were cultured with pTa and pTi6Al4V for 24 h at a density of 1×10^5/well, and a dense population of BMSCs with green fluorescence observed by fluorescence microscopy was adhered to the two groups of materials by live/dead cell staining; a few dead cells with red fluorescence were observed on the surface of the material (Figure 3B and C). Compared with pTi6Al4V, the adhesion and extension morphology of BMSCs on pTa were significantly better, indicating that pTa has better cytocompatibility than pTi6Al4V.

Proliferation of BMSCs on pTa and pTi6Al4V

BMSCs were cultured on pTa and pTi6Al4V for 1, 3, 5 and 7 days. The proliferation activity of BMSCs in the pTa group was better than that in the pTi6Al4V group at each time point, with statistical significance that increased with time: After 1−3 days, the OD values of the two groups showed a statistically significant difference at $p < 0.05$; on the 5th and 7th day, the OD values of the two groups showed a greater statistically significant difference at $p < 0.001$ (Figure 4). Therefore, we believe that pTa has a more significant ability to promote the proliferation of BMSCs than pTi6Al4V.

ALP activity assay and osteogenic mineralised nodule staining

ALP is a marker of the early differentiation of osteoblasts and plays an important role in promoting the formation of mineral elements in bone. The results showed that the expression of ALP activity in BMSCs on the pTa and pTi6Al4V surface, as well as the ALP activity of BMSCs, was increased with the prolongation of culture time. At each time point, the ALP activity trend was pTa > pTi6Al4V (Figure 5A), indicating that pTa can increase the ALP expression activity of cells and promote osseointegration at an earlier rate than pTi6Al4V.

In the process of osteogenic differentiation, mineralised nodules are the markers of osteogenic differentiation and maturity. Alizarin red staining showed mineralised nodules and deep staining were found in pTa group (B), but no obvious mineralised nodules were found in the pTi6Al4V group (C). Tetracycline staining of mineralised nodules showed there were more pink mineralised nodules in the pTa group (D) but only a few mineralised nodules in the pTi6Al4V group (E). Both results show that the number of mineralised nodules in pTa group is significantly higher than that in the pTi6Al4V group, which indicates that pTa has better ability of promoting BMSCs osteogenic differentiation than pTi6Al4V.

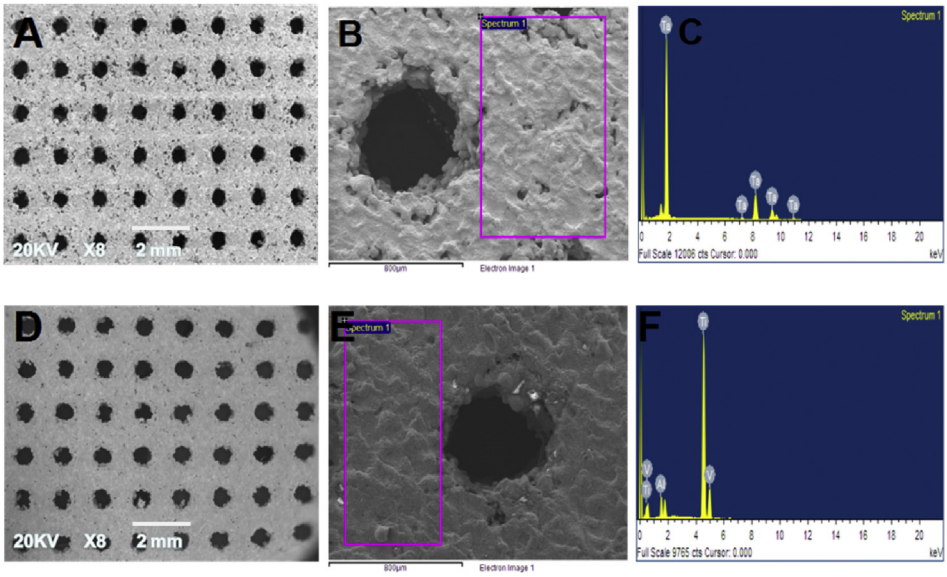

Figure 1 Scanning electron microscopy was used to observe the pore size of the two materials, and the energy spectrum was used to analyse the surface composition of the material. (A) pTa—aperture, 450—550 μm; beam width, 700—800 μm. (B and C) The surface tantalum content is 100%. (D) pTi6Al4V—aperture, 450—550 μm; beam width, 700—800 μm. (E and F) The surface titanium content is 89.85%, the Al content is 6.09% and the V content is 4.06%.

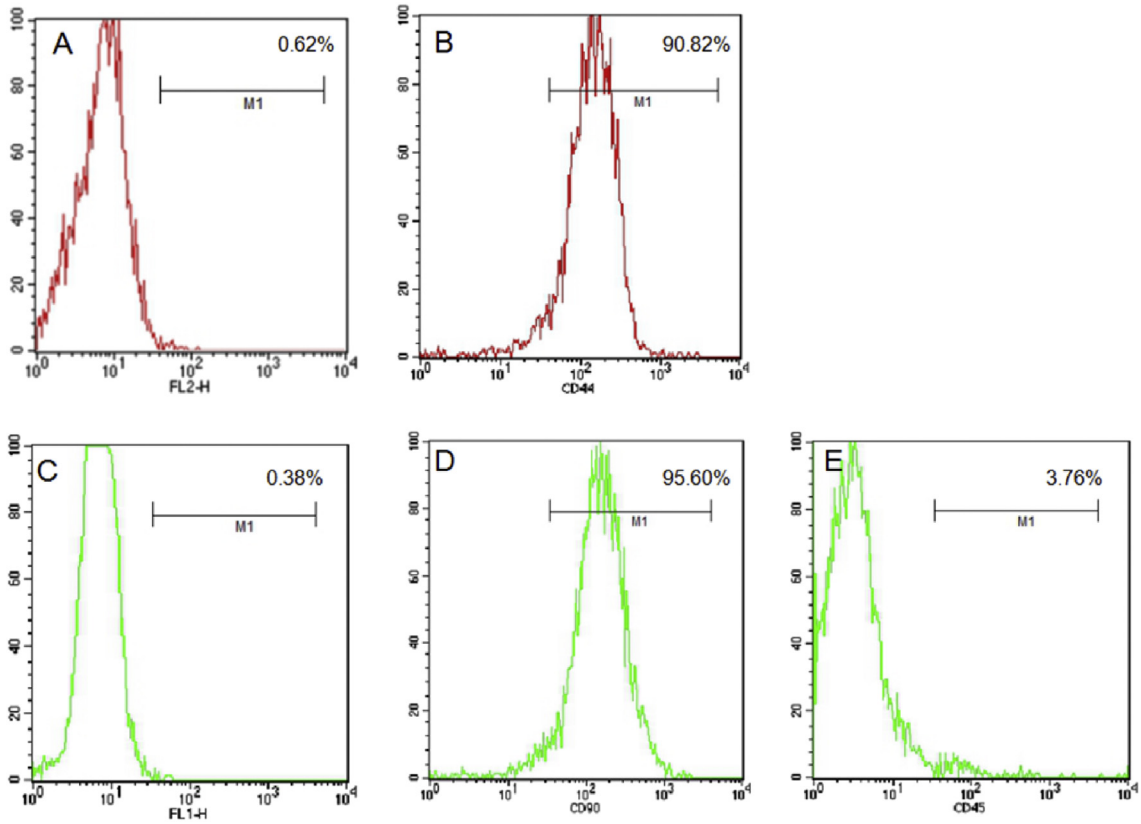

Figure 2 Identification of rat BMSCs at the third passage by flow cytometry. BMSCs were identified using the following surface markers: (A) PE negative control (0.62%), (B) CD44 (90.82%), (C) FITC negative control (0.38%), (D) CD90 (95.60%) and (E) CD45 (3.76%). BMSCs = bone marrow mesenchymal stem cells.

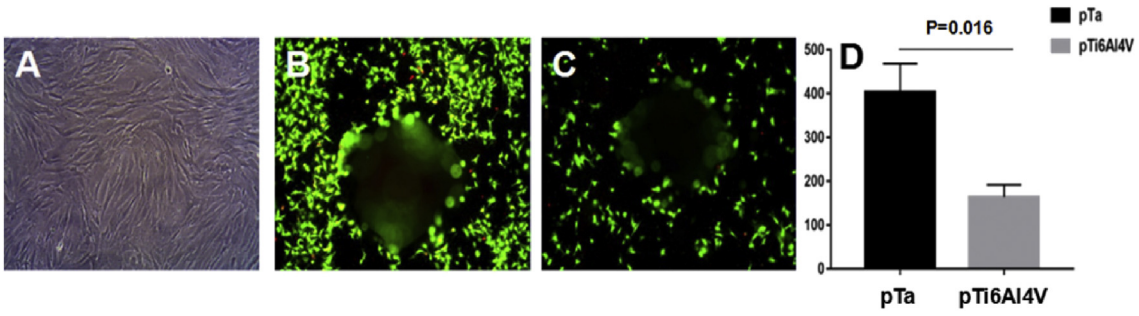

Figure 3 Adhesion of BMSCs. (A) Light microscopy image of BMSCs at the third passage. Fluorescence microscopy image of live/dead cell staining of BMSCs cocultured with the (B) pTa and (C) pTi6Al4V for 1 day. (D) Histogram after quantification of the number of adherent cells. BMSCs = bone marrow mesenchymal stem cells; pTa = porous tantalum.

Q-PCR shows the expression level of osteogenesis-related genes

The relative expression levels of ALP, OSN, Col-I, OSX and OCN were detected on the 7th, 14th and 21st day after culture of BMSCs with pTa and pTi6Al4V. Using GAPDH as the internal reference gene, the mRNA expression levels of ALP, OSN, Col-I, OSX and OCN transcription factor in the pTi6Al4V group were set as 1.00; the $2^{-\Delta\Delta Ct}$ values of ALP, OSN, Col-I, OSX and OCN gene expression in the pTa group were calculated and the relative mRNA expression levels of ALP, OSN, Col-I, OSX and OCN in the pTa group were obtained. The results showed that, except for OCN, the pTa group displayed increased expression on the 7th day and the relative mRNA expression levels of ALP, OSN, Col-I and OSX were significantly different at each time point. The relative mRNA expression levels of ALP, OSN, Col-I and OSX in the pTa group were significantly higher than those in the pTi6Al4V group. The difference in the mRNA expression between the two groups was the highest on the 7th day (Figure 6).

Western blotting shows the expression of MAPK/ERK pathway—related proteins

Western blot analysis was performed to assess whether the MAPK family members of the ERK1/2 pathway are involved in the osteogenic differentiation of BMSCs (Figure 7A). We obtained the grey values of each strip using ImageJ software (National Institutes of Health, MD, USA), the ratio of p-ERK/ERK in each group was calculated and statistical analysis was performed after repeating three experiments. The results showed that there was no significant difference in the expression of ERK1/2 and GAPDH between the two groups at 7, 14 and 21 days after culture with pTa and pTi6Al4V, but the expression of p-ERK1/2 in the pTa group was significantly increased at three time points; on the 14th day, the difference in the relative expression of p-ERK1/2 between the two groups of materials and BMSC complex was most significant (Figure 7B).

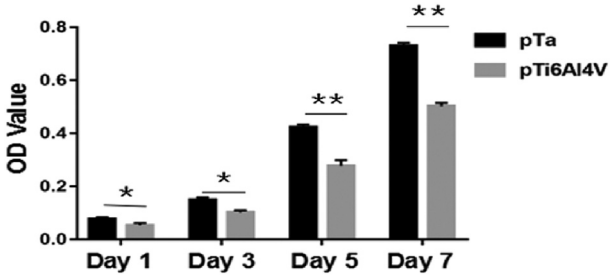

Figure 4 The CCK-8 assay was used to detect the proliferation of BMSCs after coculture with pTa and pTi6Al4V for 1, 3, 5 and 7 d (** = $p < 0.001$; * = $p < 0.05$). BMSCs = bone marrow mesenchymal stem cells; CCK-8 = cell counting kit-8; OD = optical density.

EKR1/2 inhibition study

Western blotting showed that the expression of p-ERK1/2 protein was significantly inhibited in the two groups using the MAPK/ERK—specific inhibitor U0126 compared with the untreated U0126 group (Figure 8A), and we performed quantitative calculations again. No difference was found in the expression level between the i-pTa group and i-pTi6Al4V inhibition groups (Figure 8B). After confirming the effective inhibition of the MAPK/ERK signalling pathway, Q-PCR revealed significant differences in the expression of ALP mRNA between the two inhibitory groups, but no significant difference was found in the expression of the other four genes, OSX, Col-I, OSN and OCN mRNA (Figure 8C). Therefore, we believe that pTa may be a molecular mechanism that promotes the osteogenic differentiation of BMSCs *in vitro* by activating the MAPK/ERK signalling pathway to regulate the high expression of OSX, Col-I, OSN, OCN and other osteogenic genes.

Discussion

Previous studies have shown that porous structural materials, especially those with a pore size of approximately 300—600 μm, are more conducive to cell adhesion, spreading, proliferation, differentiation and promotion of bone formation and capillaries than nonporous materials, which are formed to achieve accelerated bone necrosis, the purpose of bone defect repair and regeneration [9,26,27]. Among them, pTa, as a new type of biomedical implant material, has attracted extensive attention in the biomedical field because of its excellent biocompatibility and induction of bone formation. Ninomiya et al [28] compared the effects of different material surfaces (titanium mesh, cobalt chrome beads and pTa) on osteoblast

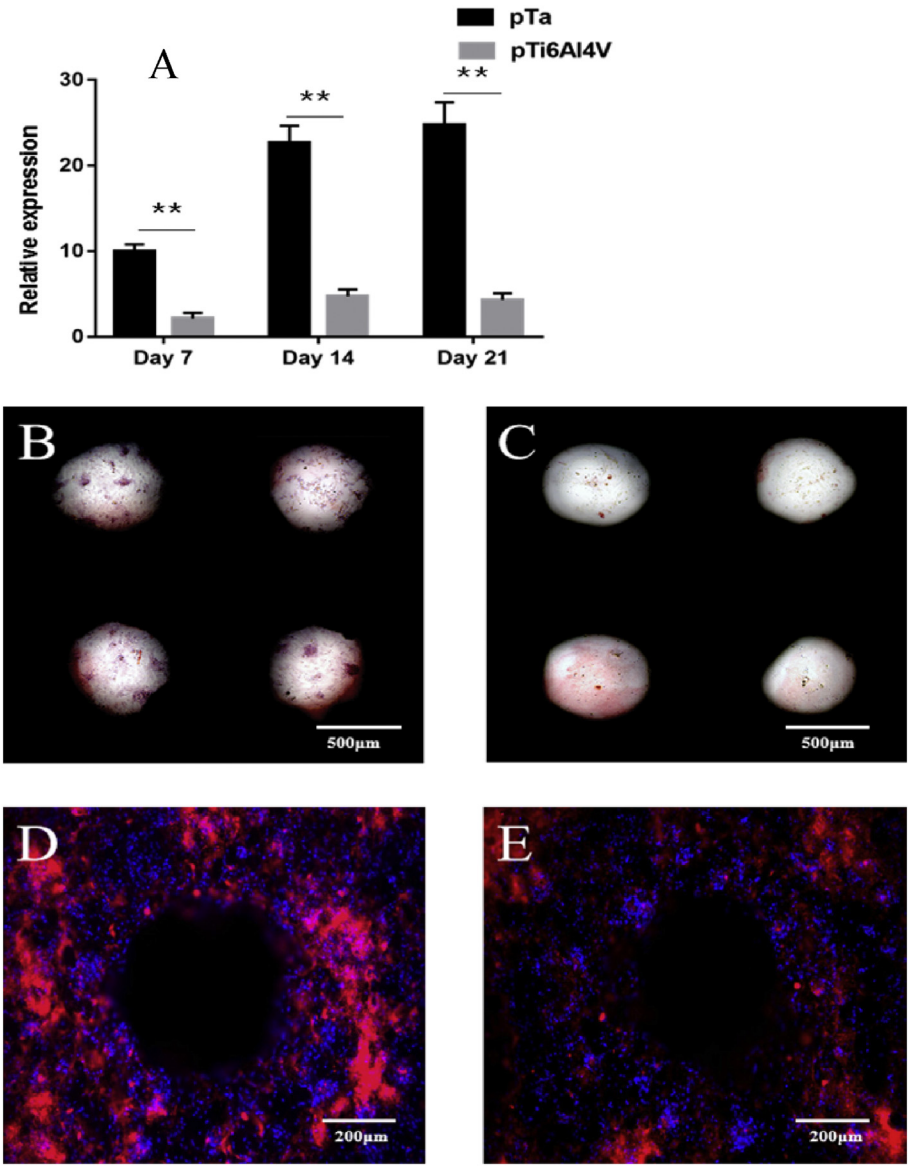

Figure 5 The ALP assay was used to detect the ALP activity of BMSCs cocultured with pTa and pTi6Al4V for 7, 14 and 21 days (A) (** = $p < 0.001$; * = $p < 0.05$); In alizarin red group, (B) mineralised nodules and deep staining were found in pTa group, (C) but no obvious mineralised nodules were found in pTi6Al4V group; (D) Tetracycline group: there were more pink mineralised nodules in pTa group, (E) but only a few mineralised nodules in pTi6Al4V group. ALP = alkaline phosphatase; BMSCs = bone marrow mesenchymal stem cells.

activity and found that the RUNX2 activity of osteoblasts on pTa was significantly greater than that on other materials. Balla et al [29] compared the ruthenium samples of the network structure with those with similar porosity, but using porous titanium samples with different pore sizes, and the results showed superior biocompatibility, similar to the experimental results we obtained. However, to date, no report has compared the osteogenic induction and molecular mechanism of pTa and pTi6Al4V with the same pore size and porosity. Our team independently developed a pTa material based on the 3D printing of pTi6Al4V combined with CVD. Scanning electron microscopy surface energy spectrum analysis showed that we produced 89.85% titanium, 6.09% Al and 4.06% pTi6Al4V, with a CVD spray thickness of approximately 20 μm and a surface Ta content of 100% pTa. We successfully produced pTa and pTi6Al4V with the same pore size and shape and studied the effects of two clinical access materials on the adhesion, proliferation and differentiation of BMSCs *in vitro* while demonstrating that the pTa material has superior biocompatibility and osteogenic differentiation performance to pTi6Al4V, exploring the molecular mechanism of pTa to promote osteogenic differentiation.

Whether *in vivo* or *in vitro*, cells and tissues will first come into contact with the surface of the material, and cell adhesion to the surface of the material is a very important step [30,31]. In this study, we found that the pTa surface has more adhesion capability to BMSCs than pTi6Al4V by the

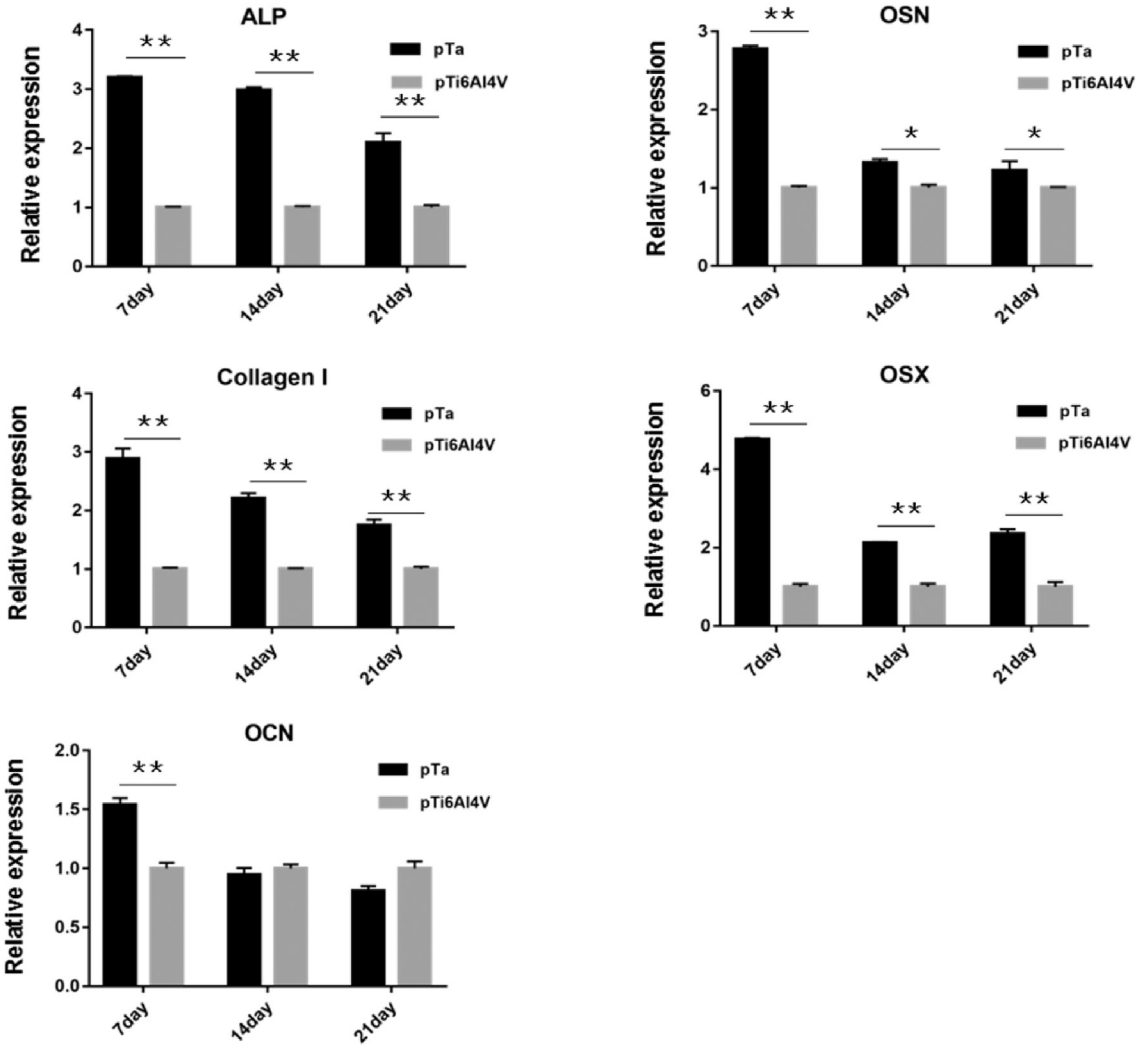

Figure 6 The mRNA expression of osteogenic genes of BMSCs cocultured with pTa and pTi6Al4V for 7, 14 and 21 days (** = $p < 0.001$; * = $p < 0.05$). ALP = alkaline phosphatase; BMSCs = bone marrow mesenchymal stem cells; OSX = osterix; OSN = osteonectin; OCN = osteocalcin; pTa = porous tantalum.

live—dead cell staining assay. This result proves that the pTa has significantly superior biology to pTi6Al4V with the same porous structure. Compatibility also indicates that the Ta metal is a high-quality material based on the same porous structure. The adhesion of a large number of cells in the early stage is precisely an important advantage of the clinical application of pTa implants combined with autologous BMSCs in the treatment of osteonecrosis and bone defects. The amount of cell adhesion in the early stage of the implant material not only affects the survival rate of autografted BMSCs but also determines the efficiency of proliferation and differentiation [32].

Thereafter, we used the CCK-8 assay to evaluate that the proliferation of BMSCs in the two groups was significantly different at 1, 3, 5 and 7 days. The proliferation activity of BMSCs in the pTa group was significantly better than that in the pTi6Al4V group. In this study, we plated the same number of cells in 12-well plates with pTa and pTi6Al4V, and OD measurements were taken on 1, 3, 5 and 7 days. The results showed that the OD values of the two groups were significantly different at each time point, and the difference became increasingly significant with the prolongation of the culture time. This result also showed that the pTa material has better biocompatibility than pTi6Al4V and can promote the proliferation of stem cells on the surface ($P < 0.05$). This performance in autologous BMSCs combined with pTa implantation for the treatment of osteonecrosis, bone defects and other diseases will play an important role in early efficacy.

An important finding of this study was that the pTa materials we produced exhibited significant osteogenic differentiation of BMSCs compared with pTi6Al4V. The ALP activity assay showed that the ALP activity of BMSCs in the pTa group was significantly increased. The high expression of ALP activity was an early marker of osteoblast differentiation and maturation. The quantitative detection of ALP can reflect the differentiation level of osteoblasts. The more obvious the differentiation of mature osteoblasts, the stronger the ALP activity, enhanced bone formation and promotion of bone matrix mineralisation; thus, the activity

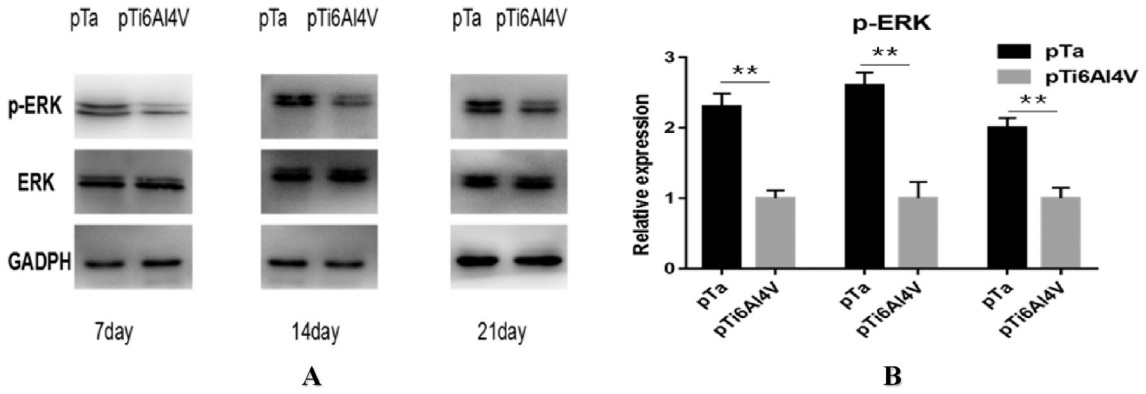

Figure 7 Q-PCR. (A) p-ERK and ERK protein expression of BMSCs cocultured with pTa and pTi6Al4V for 7, 14 and 21 days, GAPDH as an internal reference. (B) A p-ERK quantitative histogram based on imaging analysis of the Western blot bands (** = $p < 0.001$; * = $p < 0.05$). BMSCs = bone marrow mesenchymal stem cells; Q-PCR = real-time quantitative polymerase chain reaction.

of ALP is a good indicator that reflects the degree of differentiation and functional status of osteoblasts [33,34]. In the results of subsequent Q-PCR, the expression levels of the osteogenic genes ALP, OSX, Col-I, OSN and OCN of BMSCs in the pTa group were significantly increased compared with those in the pTi6Al4V group. At the early time of 7 days, the aforementioned five osteogenic genes were significantly increased. At 14 and 21 days, except for OCN, the expression levels of other four genes were still significantly elevated. ALP, OSX, Col-I, OSN and OCN are all important and specific indicators reflecting the level of osteogenic differentiation [33,35—37].

At the same time, we found that pTa can regulate the molecular mechanism of the osteogenic differentiation of BMSCs *in vitro* by activating the MAPK/ERK signalling pathway to regulate the high expression of OSX, Col-I, OSN, OCN and other osteogenic genes. Western blotting analysis showed that p-ERK, which is an effector protein in the MAPK/ERK signalling pathway, is significantly expressed in the pTa group after culture with the two groups of

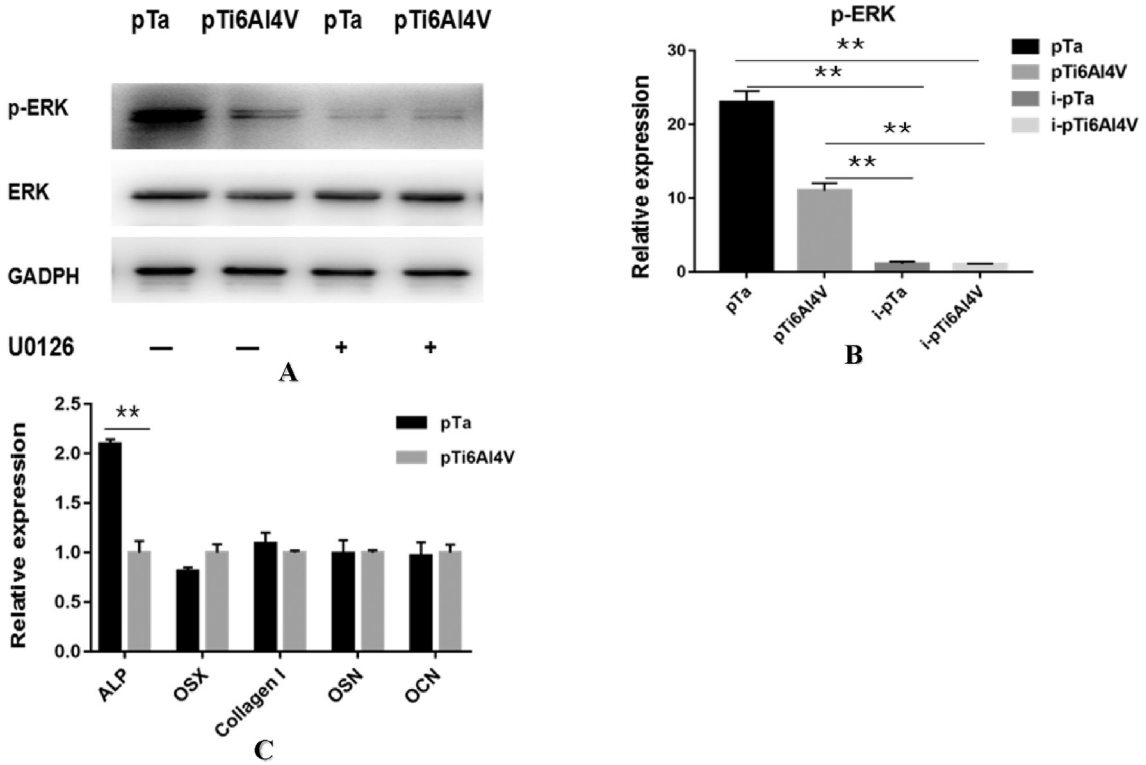

Figure 8 Western blotting and Q-PCR. (A) After application of the inhibitor U0126, BMSCs were cocultured with pTa and pTi6Al4V for 7 days, and p-ERK, ERK and GAPDH immunoblotting was performed. (B) p-ERK quantitative histogram based on imaging analysis of the Western blot bands. (C) Q-PCR results of the relative expression of the indicated osteogenic genes (** = $p < 0.001$; * = $p < 0.05$). BMSCs = bone marrow mesenchymal stem cells; Q-PCR = real-time quantitative polymerase chain reaction.

materials. Then, we used a suitable concentration of U0126 (a selective inhibitor of the MAPK/ERK signalling pathway) mixed with the medium for the culture of the material cell complex. The expression of p-ERK was inhibited after the MAPK/ERK signalling pathway was inhibited [38—40], and the expression levels of ERK protein were not affected. Q-PCR revealed significant differences in the two component bone genes except ALP. The expression of the four genes OSX, Col-I, OSN and OCN was changed from significantly increased to no significant difference. This finding suggests that the activation of the MAPK/ERK signalling pathway may play an important role in the molecular mechanism of the osteoblast differentiation of BMSCs in pTa: pTa activates the MAPK/ERK signalling pathway, increasing the expression of its effector protein p-ERK, which regulates OSX, Col-I, OSN, OCN and other osteogenic genes by increasing their expression to promote the *in vitro* osteogenic differentiation of BMSCs. Further study will focus on the exact relationship between the four genes OSX, Col-I, OSN and OCN and the MAPK/ERK signalling pathway.

In summary, we found that compared with pTi6Al4V with the same pore size, pTa can promote BMSC adhesion growth and osteogenic differentiation—that is, superior biocompatibility and osteoinductive ability—enhancing the effectiveness of bone healing *in vivo*. At the same time, most importantly, we found that pTa may regulate the molecular expression of OSX, Col-I, OSN, OCN and other osteogenic genes by activating the MAPK/ERK signalling pathway to promote the osteogenic differentiation of BMSCs *in vitro*. This will also provide a theoretical basis for the application of pTa implant materials in orthopaedics and other fields. Another point worthy of our attention is that our self-developed pTa material produced by 3D printing combined with the CVD method not only retains excellent biological activity and osteoinductive ability of the original Ta metal but also saves considerably on material costs to achieve mass production of personalised orthopaedic implants with pTa as a stent and to accelerate the wide application of pTa implants in clinical practice, which have certain profound significance.

Conflicts of interest statement

The authors have no conflicts of interest to disclose in relation to this article.

Funding

The project was supported by the National Natural Science Foundation of China (No. 81672139&81601885), PhD Start-up Fund Guidance Program (20170520015), Science and Technology Innovation Fund of Dalian (2018J11CY030) and Dalian Science and Technology Bureau Project (2017RQ153).

References

[1] Mont MA, Jones LC, Hungerford DS. Nontraumatic osteonecrosis of the femoral head: ten years later. J Bone Jt Surg Am Vol 2006;88:1117—32.

[2] Rackwitz L, Eden L, Reppenhagen S, Reichert JC, Jakob F, Walles H, et al. Stem cell- and growth factor-based regenerative therapies for avascular necrosis of the femoral head. Stem Cell Res Ther 2012;3:7.

[3] Zhang W, Chang Q, Xu L, Li G, Yang G, Ding X, et al. Graphene oxide-copper nanocomposite-coated porous CaP scaffold for vascularized bone regeneration via activation of hif-1alpha. Adv Healthc Mater 2016;5:1299—309.

[4] Langer R, Vacanti JP. Tissue engineering. Science 2000;260:920—6.

[5] Li Z, Kawashita M. Current progress in inorganic artificial biomaterials. J Artif Organs Off J Jpn Soc Artif Organs 2011;14:163—70.

[6] Sehatzadeh S, Kaulback K, Levin L. Metal-on-metal hip resurfacing arthroplasty: an analysis of safety and revision rates. Ontario Health Technol Assess Ser 2012;12:1—63.

[7] Disegi JA, Eschbach L. Stainless steel in bone surgery. Inj Int J Care Inj 2000;31:D2—6.

[8] Herranz-Diez C, Gil FJ, Guillem-Marti J. Mechanical and physicochemical characterization along with biological interactions of a new Ti25Nb21Hf alloy for bone tissue engineering. J Biomater Appl 2015;30:171—81.

[9] Banerjee S, Issa K, Kapadia BH, Pivec R, Khanuja HS, Mont MA, et al. Systematic review on outcomes of acetabular revisions with highly-porous metals. Int Orthop 2014;38:689—702.

[10] Zhao D, Zhang Y, Wang W, Liu Y, Li Z, Wang B, et al. Tantalum rod implantation and vascularized iliac grafting for osteonecrosis of the femoral head. Orthopedics 2013;36:789—95.

[11] Garbuz DS, Hu Y, Kim WY, Duan K, Masri BA, Oxland TR, et al. Enhanced gap filling and osteoconduction associated with alendronate-calcium phosphate-coated porous tantalum. J Bone Jt Surg Am Vol 2008;90:1090—100.

[12] Bobyn JD, Toh KK, Hacking SA, Tanzer M, Krygier JJ. Tissue response to porous tantalum acetabular cups: a canine model. J Arthroplast 1999;14:347—54.

[13] Li M, Ikehara S. Bone-marrow-derived mesenchymal stem cells for organ repair. Stem Cell Int 2013;2013:132642 (2013-3-11) 2013.

[14] Lee RH, Kim B, Choi I, Kim H, Choi HS, Suh K, et al. Characterization and expression analysis of mesenchymal stem cells from human bone marrow and adipose tissue. Cell Physiol Biochem Int J Exp Cell Physiol Biochem Pharmacol 2004;14:311—24.

[15] Zhao D, Cui D, Wang B, Tian F, Guo L, Yang L, et al. Treatment of early stage osteonecrosis of the femoral head with autologous implantation of bone marrow-derived and cultured mesenchymal stem cells. Bone 2012;50:325—30.

[16] Wei X, Zhao D, Wang B, Wang W, Kang K, Xie H, et al. Tantalum coating of porous carbon scaffold supplemented with autologous bone marrow stromal stem cells for bone regeneration in vitro and in vivo. Exp Biol Med 2016;241:592—602.

[17] Chen Z, Wu C, Gu W, Klein T, Crawford R, Xiao Y. Osteogenic differentiation of bone marrow MSCs by β-tricalcium phosphate stimulating macrophages via BMP2 signalling pathway. Biomaterials 2014;35:1507—18.

[18] Zhao D, Liu B, Wang B, Yang L, Xie H, Huang S, et al. Autologous bone marrow mesenchymal stem cells associated with tantalum rod implantation and vascularized iliac grafting for the treatment of end-stage osteonecrosis of the femoral head. BioMed Res Int 2015;2015:240506.

[19] Chen Z, Gibson TB, Robinson F, Silvestro L, Pearson G, Xu B, et al. MAP kinases - chemical reviews (ACS Publications). American Chemical Society.

[20] Jaiswal RK, Jaiswal N, Bruder SP, Mbalaviele G, Marshak DR, Pittenger MF. Adult human mesenchymal stem cell differentiation to the osteogenic or adipogenic lineage is regulated by

mitogen-activated protein kinase. J Biol Chem 2000;275:9645—52.
[21] Zhang P, Dai Q, Ouyang N, Yang X, Wang J, Zhou S, et al. Mechanical strain promotes osteogenesis of BMSCs from ovariectomized rats via the ERK1/2 but not p38 or JNK-MAPK signaling pathways. Curr Mol Med 2015;15.
[22] Cao H, Zhang W, Meng F, Guo J, Wang D, Qian S, et al. Osteogenesis catalyzed by titanium-supported silver nanoparticles 2017;9:5149—57.
[23] Xu M, Peng D. Mesenchymal stem cells cultured on tantalum used in early-stage avascular necrosis of the femoral head. Med Hypotheses 2011;76:199—200.
[24] Rosalbino F, Maccio D, Giannoni P, Quarto R, Saccone A. Study of the in vitro corrosion behavior and biocompatibility of Zr-2.5Nb and Zr-1.5Nb-1Ta (at%) crystalline alloys. J Mater Sci Mater Med 2011;22:1293—302.
[25] Ma Z, Xie H, Wang B, Wei X, Zhao D. A novel Tantalum coating on porous SiC used for bone filling material. Mater Lett 2016;179:166—9.
[26] Jones AC, Arns CH, Sheppard AP, Hutmacher DW, Milthorpe BK, Knackstedt MA. Assessment of bone ingrowth into porous biomaterials using MICRO-CT. Biomaterials 2007;28:2491—504.
[27] Gotz HE, Muller M, Emmel A, Holzwarth U, Erben RG, Stangl R. Effect of surface finish on the osseointegration of laser-treated titanium alloy implants. Biomaterials 2004;25:4057—64.
[28] Ninomiya JT, Struve JA, Krolikowski J, Hawkins M, Weihrauch D. Porous ongrowth surfaces alter osteoblast maturation and mineralization. J Biomed Mater Res A 2015;103:276—81.
[29] Balla VK, Bodhak S, Bose S, Bandyopadhyay A. Porous tantalum structures for bone implants: fabrication, mechanical and in vitro biological properties. Acta Biomater 2010;6:3349—59.
[30] Sawyer AA, Hennessy KM, Bellis SL. Regulation of mesenchymal stem cell attachment and spreading on hydroxyapatite by RGD peptides and adsorbed serum proteins. Biomaterials 2005;26:1467—75.
[31] Gharizadeh N, Moradi K, Haghighizadeh MH. A study of microleakage in Class II composite restorations using four different curing techniques. Operat Dent 2007;32:336—40.
[32] Anselme K. Osteoblast adhesion on biomaterials. Biomaterials 2000;21:667—81.
[33] Kojima H, Fujimiya M, Matsumura K, Nakahara T, Hara M, Chan L. Extrapancreatic insulin-producing cells in multiple organs in diabetes. Proc Natl Acad Sci U S A 2004;101:2458—63.
[34] Canturk Z, Canturk NZ, Cetinarslan B, Senturk O, Ercin C, Yenise C. Effect of G-CSF on ethanol-induced hemorrhagic gastritis model in diabetes mellitus-induced rats. Endocr Res 2001;27:191—201.
[35] Wang N, Li H, Wang J, Chen S, Ma Y, Zhang Z. Study on the anticorrosion, biocompatibility, and osteoinductivity of tantalum decorated with tantalum oxide nanotube array films. ACS Appl Mater Interfaces 2012;4. 4516-452.
[36] Tognarini I, Sorace S, Zonefrati R, Galli G, Gozzini A, Carbonell Sala S, et al. In vitro differentiation of human mesenchymal stem cells on Ti6Al4V surfaces. Biomaterials 2008;29:809—24.
[37] Lim TY, Wang W, Shi Z, Poh CK, Neoh KG. Human bone marrow-derived mesenchymal stem cells and osteoblast differentiation on titanium with surface-grafted chitosan and immobilized bone morphogenetic protein-2. J Mater Sci Mater Med 2009;20:1—10.
[38] Zhou Y, Guan X, Wang H, Zhu Z, Li C, Wu S, et al. Hypoxia induces osteogenic/angiogenic responses of bone marrow-derived mesenchymal stromal cells seeded on bone-derived scaffolds via ERK1/2 and p38 pathways. Biotechnol Bioeng 2013;110:1794—804.
[39] Wang Y, Li J, Song W, Yu J. Mineral trioxide aggregate upregulates odonto/osteogenic capacity of bone marrow stromal cells from craniofacial bones via JNK and ERK MAPK signalling pathways. Cell Prolif 2014;47:241—8.
[40] Hu J, Liao H, Ma Z, Chen H, Huang Z, Zhang Y, et al. Focal adhesion kinase signaling mediated the enhancement of osteogenesis of human mesenchymal stem cells induced by extracorporeal shockwave. Sci Rep 2016;6:20875.